Ultrasensitivity and noise amplification in a model of V. harveyi quorum sensing

Paul C. Bressloff

Phys. Rev. E **93**, 062418 — Published 28 June 2016

DOI: 10.1103/PhysRevE.93.062418

Ultrasensitivity and noise amplification in a model of *V. harveyi* quorum sensing

Paul C. Bressloff[1]
[1] *Department of Mathematics, University of Utah, 155 South 1400 East, Salt Lake City UT 84112*

We analyze ultrasensitivity in a model of *V. harveyi* quorum sensing. We consider a feedforward model consisting of two biochemical networks per cell. The first represents the interchange of a signaling molecule (autoinducer) between the cell cytoplasm and an extracellular domain, and the binding of intracellular autoinducer to cognate receptors. The unbound and bound receptors within each cell act as kinases and phosphotases, respectively, which then drive a second biochemical network consisting of a phosphorylation-dephosphorylation cycle. We ignore subsequent signaling pathways associated with gene regulation and the possible modification in the production rate of autoinducer (positive feedback). We show how the resulting quorum sensing system exhibits ultrasensivity with respect to changes in cell density. We also demonstrate how quorum sensing can protect against the noise amplification of fast environmental fluctuations in comparison to a single isolated cell.

PACS numbers: 87.10.-e, 87.18.Fx, 87.18.Mp, 05.40.-a

I. INTRODUCTION

Quorum sensing is a form of system stimulus and response that is correlated to population density. Many species of bacteria use quorum sensing to coordinate various types of behavior including bioluminescence, biofilm formation, virulence, and antibiotic resistance, based on the local density of the bacterial population [1–8]. In an analogous fashion, some social insects use quorum sensing to determine where to nest [9]. Roughly speaking, quorum sensing can function as a decision-making process in any decentralized system, provided that individual components have some mechanism for determining the number or density of the population and a stereotypical response once some density threshold has been reached.

In the case of bacteria, quorum sensing involves the production and extracellular secretion of certain signaling molecules called *autoinducers*. Each cell also has receptors that can specifically detect the signaling molecule via ligand-receptor binding, which then activates transcription of certain genes, including those for inducer synthesis. However, since there is a low likelihood of an individual bacterium detecting its own secreted inducer, the cell must encounter signaling molecules secreted by other cells in its environment in order for gene transcription to be activated. When only a few other bacteria of the same kind are in the vicinity (low bacterial population density), diffusion reduces the concentration of the inducer in the surrounding medium to almost zero, resulting in small amounts of inducer being produced. On the other hand, as the population grows, the concentration of the inducer passes a threshold, causing more inducer to be synthesized. This generates a positive feedback loop that fully activates the receptor, and induces the up-regulation of other specific genes. Hence, all of the cells initiate transcription at approximately the same time, resulting in some form of coordinated behavior. The basic process at the single-cell level is shown in Fig. 1.

Most models of bacterial quorum sensing are based on deterministic ordinary differential equations (ODEs), in which both the individual cells and the extracellular medium are treated as well-mixed compartments (fast diffusion limit) [10–18]. (Examples of spatial models can be found in Refs. [12, 19–22].) From a dynamical systems perspective, two distinct forms of collective behavior are typically considered: either the population acts as a biochemical switch [12] or as a synchronized biochemical oscillator [14, 17, 18]. In this paper, we focus on the former. At least two distinct mechanisms for a biochemical switch have been identified. The first mechanism involves the occurrence of bistability in a gene regulatory network, as exemplified by the mathematical model of quorum sensing in the bacterium *Pseudomonas aeruginosa* developed by Dockery and Keener [12]. *P. aeruginosa* is a human pathogen that monitors its cell density in order to control the release of various virulence factors [2, 3]. That is, if a small number of bacteria released toxins then this could easily be neutralized by an efficient host response, whereas the effectiveness of the response would be considerably diminished if toxins were only released after the bacterial colony has reached a critical size via quorum sensing. Multiple steady-steady states have also been found in a related ODE model of quorum sensing in the bioluminescent bacteria *V. fisheri* [10]. In this system, quorum sensing limits the production of bioluminescent luciferase to situations where cell populations are large; this saves energy since the signal from a small number of cells would be invisible and thus useless.

Recent experimental studies of quorum sensing in the bacterial species *V. harveyi* and *V. cholerae* [4, 6, 7] provide evidence for an alternative switching mechanism, which can provide robust switch-like behavior without bistability. In these quorum sensing systems two or more parallel signaling pathways control a gene regulatory network via a cascade of phosphorylation-dephosphorylation cycles (PdPCs). PdPCs are a very common signaling mechanism within cells, consisting of a protein that can exist in an unmodified (unphosphorylated) or a modi-

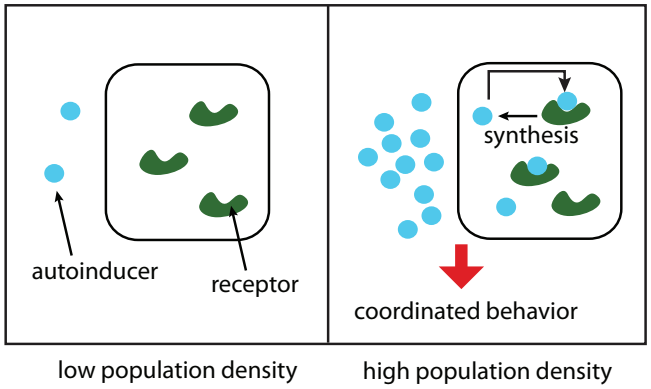

FIG. 1. (Color online) A schematic illustration of quorum sensing at the single-cell level.

fied (phosphorylated) state. Interconversion of the inactivated and activated protein states is catalyzed by two enzymes, *kinases* that phosphorylate the inactivated protein and *phosphotases* that dephopshorylate the activated protein. Within the context of quorum sensing, the binding of an autodinducer to its cognate receptor switches the receptor from acting like a kinase to one acting like a phosphotase. Thus the PdPCs are driven by the level of autoinducer which itself depends on the cell density. One characteristic feature of a PdPC is that it exhibits *ultrasenstivity*, that is, its response to a stimulus takes the form of a sharp, switch-like sigmoid function [23–27].

In this paper, we analyze ultrasensitivity in *V. harveyi* quorum sensing. For simplicity, we focus on a single phosphorylation pathway by adapting the Goldbeter-Koshland of phosphorylation-dephosphorylation cycles [23]. We consider a feedforward model consisting of two biochemical networks per cell. The first represents the interchange of an autoinducer between the cytoplasm and an extracellular domain, and the binding of intracellular autoinducer to cognate receptors. The unbound and bound receptors within each cell act as kinases and phosphotases, respectively, which then drive a second biochemical network consisting of a PdPC. We ignore subsequent signaling pathways associated with gene regulation and the possible modification in the production rate of autoinducer (positive feedback). We show how the resulting quorum sensing system can exhibit ultrasensivity with respect to changes in cell density. However, the resulting switch-like behavior can make the system vulnerable to fast fluctuations in the environment, which could be detrimental. Therefore, we also demonstrate how quorum sensing can protect against the noise amplification of fast fluctuations in comparison to the PdPC of a single isolated cell.

The structure of the paper is as follows. In Sec. II we consider a general ODE model of quorum sensing and derive conditions for the global convergence of the system. Our basic model of quorum sensing in *V. harveyi* is presented in Sec. III, where we prove global convergence of the model equations and use this to establish ultrasensitivity with respect to population density. In Sec. IV we address the issue of noise amplification in the presence of receptor fluctuations, and show how quorum sensing suppresses the effects of noise.

II. DIFFUSIVELY COUPLED MODEL OF QUORUM SENSING

We begin by formulating a general model of quorum sensing and analyzing the global convergence properties of the model using the contraction theory tools of Russo and Slotine [28]. Suppose that there are N cells labeled $i = 1, \ldots, N$. Let $U(t)$ denote the concentration of signaling molecule in the extracellular space and let u_i be the corresponding intracellular concentration within the i-th cell. Suppose that there are K other chemical species within each cell, which together with the signaling molecule comprise a regulatory network. Let $\mathbf{v}_i = (v_{i,1}, \ldots, v_{i,K})$ with $v_{i,k}$ the concentration of species k within the i-th cell. A deterministic model of quorum sensing can then be written in the general form [14]

$$\frac{du_i}{dt} = F(u_i, \mathbf{v}_i) - \kappa(u_i - U), \quad i = 1, \ldots, N \tag{2.1a}$$

$$\frac{dv_{i,k}}{dt} = G_k(u_i, \mathbf{v}_i), \quad k = 1, \ldots, K \tag{2.1b}$$

$$\frac{dU}{dt} = \frac{\alpha\kappa}{N}\sum_{j=1}^{N}(u_j - U) - \gamma U, \tag{2.1c}$$

Here $F(u, \mathbf{v})$ and $G_k(u, \mathbf{v})$ are the reaction rates of the regulatory network based on mass action kinetics, the term $\kappa(u_j - U)$ represents the diffusive exchange of signaling molecules across the membrane of the j-th cell with diffusive conductance κ, and γ is the rate of degradation of extracellular signaling molecules. Finally, $\alpha = V_{\rm cyt}/V_{\rm ext}$ is a cell density parameter equal to the ratio of the total cytosolic and extracellular volume. Note that $V_{\rm cyt} = v_{\rm cyt}N$, where $v_{\rm cyt}$ is the single-cell volume. In this paper we treat N and α as independent variables.

The global convergence properties of quorum sensing networks, where coupling between nodes in the network is mediated by a common environmental variable, has been analyzed within the context of nonlinear dynamical systems in Ref. [28]. These authors consider a more general class of model than given by Eqs. (2.1), including non-diffusive coupling and non-identical cells. In order to develop our model of ultrasensitivity in *V. harveyi* quorum sensing, it is useful to apply the analysis of Ref. [28] to the system of Eqs. (2.1). This requires recalling some basic results of nonlinear contraction theory [29]. Consider the m-dimensional dynamical system

$$\frac{d\mathbf{x}}{dt} = \mathbf{f}(\mathbf{x}, t), \quad \mathbf{x} \in \mathbb{R}^n, \tag{2.2}$$

with $\mathbf{f} : \mathbb{R}^n \to \mathbb{R}^n$ a smooth nonlinear vector field. Introduce the vector norm $|x|$ for $x \in \mathbb{R}^n$ and let $\|A\|$ be the

induced matrix norm for an arbitrary square matrix A, that is,

$$\|A\| = \sup\{|A\mathbf{x}| : \mathbf{x} \in R^n \text{ with } |\mathbf{x}| = 1\}.$$

Some common examples are as follows:

$$|\mathbf{x}|_1 = \sum_{j=1}^{n} |x_j|, \quad \|A\|_1 = \max_{1\le j\le n} \sum_{i=1}^{n} |a_{ij}|,$$

$$|\mathbf{x}|_2 = \left(\sum_{j=1}^{n} |x_j|^2\right)^{1/2}, \quad \|A\|_2 = \sqrt{\lambda_{\max}(A^*A)}$$

$$|\mathbf{x}|_\infty = \max_{1\le j\le n} |x_j|, \quad \|A\|_\infty = \max_{1\le i\le n} \sum_{j=1}^{n} |a_{ij}|,$$

where A^* is the transpose of A and $\lambda_{\max}(A^*A)$ is the largest eigenvalue of the positive semi-definite matrix A^*A. Define the associated matrix measure μ as

$$\mu(A) = \lim_{h\to 0^+} \frac{1}{h}(\|I + hA\| - 1),$$

where I is the identity matrix. For the three above norms on $\mathbb{R}^n$, the associated matrix measures are

$$\mu_1(A) = \max_{1\le j\le n} \{a_{jj} + \sum_{i\ne j} |a_{ij}|\}$$

$$\mu_2(A) = \max_{1\le i\le n} \{\lambda_i([A + A^*]/2)\}$$

$$\mu_\infty(A) = \max_{1\le i\le n} \{a_{ii} + \sum_{j\ne i} |a_{ij}|\}.$$

Given these definitions, the basic contraction theorem is as follows [28]:

Theorem 1 *The n-dimensional dynamical system (2.2) is said to be contracting if any two trajectories, starting from different initial conditions, converge exponentially to each other. A sufficient condition for a system to be contracting is the existence of some matrix measure μ for which there exists a constant $\lambda > 0$ such that*

$$\mu(J(\mathbf{x}, t)) \le -\lambda, \quad J_{ij} = \frac{\partial f_i}{\partial x_j} \tag{2.3}$$

for all $\mathbf{x}, t$. The scalar λ defines the rate of contraction.

A related concept is *partial contraction* [28]. Consider a smooth nonlinear dynamical system of the form $\dot{\mathbf{x}} = f(\mathbf{x}, \mathbf{x}, t)$ with $\mathbf{x} \in \mathbb{R}^n$. Suppose that the so-called virtual non-autonomous system $\dot{\mathbf{y}} = f(\mathbf{y}, \mathbf{x}, t)$ with $\mathbf{x}(t)$ evolving as specified, is contracting with respect to $\mathbf{y}$. If a particular solution of the virtual system has some smooth specific property, then all trajectories of the original x system exhibit the same property in the large t limit. This follows from the fact that $\mathbf{y}(t) = \mathbf{x}(t)$, $t \ge 0$, is another particular solution of the virtual system, and all trajectories of the $\mathbf{y}$ system converge exponentially to a single trajectory.

In order to apply the above results to Eqs. (2.1), we rewrite the latter in the form

$$\frac{d\mathbf{x}_i}{dt} = \mathbf{f}(\mathbf{x}_i) - \kappa((\mathbf{x}_i)_1 - U)\mathbf{e}_1, \quad i = 1, \ldots, N \tag{2.4a}$$

$$\frac{dU}{dt} = \frac{\alpha\kappa}{N} \sum_{j=1}^{N} ((\mathbf{x}_j)_1 - U) - \gamma U, \tag{2.4b}$$

with $\mathbf{x}_i = (u_i, \mathbf{v}_i) \in \mathbb{R}^{1+K}$, $(\mathbf{x}_i)_1 = u_i$, $\mathbf{f} = (F, G_1, \ldots, G_K)$ and $\mathbf{e}_1 = (1, 0, \ldots, 0)$. From the contraction theorem and the notion of partial contraction, one can show that the global convergence condition

$$|\mathbf{x}_i(t) - \mathbf{x}_j(t)| \to 0 \text{ as } t \to \infty$$

holds provided that $\mathbf{f}(\mathbf{x}) - \kappa(\mathbf{x})_1\mathbf{e}_1$ is contracting. The proof follows from considering the reduced order virtual system

$$\dot{\mathbf{y}} = \mathbf{f}(\mathbf{y}) - \kappa(\mathbf{y})_1\mathbf{e}_1 + \kappa U(t)\mathbf{e}_1,$$

where $U(t)$ is treated as an external input. Setting $\mathbf{y}(y) = \mathbf{x}_i(t)$ in the virtual system recovers the dynamics of the ith cell. Hence, $\mathbf{x}_i(t)$ for $i = 1, \ldots, N$ are particular solutions of the virtual system so that if the virtual system is contracting in $\mathbf{y}$, then all of its solutions converge exponentially toward each other, including the solutions $x_i(t)$. In this asymptotic limit, we effectively have a single cell diffusively coupled to the extracellular medium, that is $u_i(t) \to u(t)$ and $\mathbf{v}_i(t) \to \mathbf{v}(t)$ with:

$$\frac{du}{dt} = F(u, \mathbf{v}) - \kappa(u - U), \tag{2.5a}$$

$$\frac{dv_k}{dt} = G_k(u, \mathbf{v}), \tag{2.5b}$$

$$\frac{dU}{dt} = \alpha\kappa(u - U) - \gamma U. \tag{2.5c}$$

III. ULTRASENSITIVITY IN *V. HARVEYI* QUORUM SENSING

The bioluminescent bacterium *V. harveyi* has three parallel quorum sensing systems, each consisting of a distinct autoinducer (HAI-1, AI-2, CAI-1), cognate receptor (LuxN, LuxP/Q, CqS), and associated enzyme (LuxM, LuxS, CqsA) that helps produce the autoinducer, see Fig. 2. (The human pathogen *V. cholerae* has a similar quorum sensing network, except there appear to be only two parallel pathways. Note, however, that a recent study suggests there could be up to four parallel pathways [30].) Each autoinducer moves freely between the intracellular and extracellular domains. At low cell densities there are relatively low levels of autinducer due to diffusion, so that there is a low probability that the autoinducer can bind to its cognate receptor. Consequently, the receptor acts as a kinase that autophosphorylates, and subsequently transfers its phosphate to the

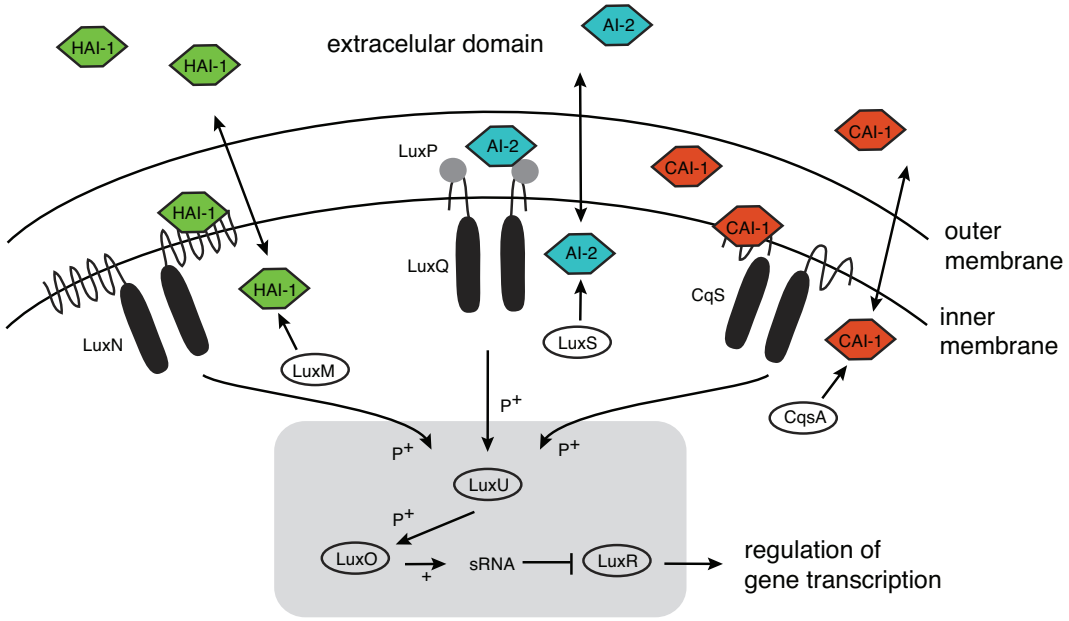

FIG. 2. (Color on-line) Summary of the *V. harveyi* quorum sensing circuit. Three phosphorylation cascades work in parallel to control the ratio of LuxO to LuxO-P based on local cell-population density. Five sRNA, qrr1-5, then regulate expression of quorum sensing target genes including the master transcriptional regulator LuxR, which upregulates downstream factors.

cytoplasmic protein LuxU. LuxU-P then passes its phosphate to the DNA-binding regulatory protein LuxO to yield LuxO-P. The upshot is that at low cell densities, the ratio of [LuxO-P] to [LuxO] is high and this activates transcription of the genes encoding five regulatory *small RNAs* (sRNAs) termed Qrr1-Qrr5 (Quorum Regulatory RNA). Bacterial sRNAs are small (50-250 nucleotide) non-coding RNA molecules that can either bind to a protein and alter its function or bind to mRNA and regulate gene expression. In the case of quorum sensing in *V. harveyi*, the small sRNAs Qrr1–Qrr5 destabilize the transcriptional activator protein LuxR, thus preventing the activation of target genes responsible for the production of various proteins, including bioluminescent luciferase. Hence, at low cell density the bacteria do not bioluminesce. On the other hand, at high cell density, the concentration of intracellular autodinducers is increased so that they have a higher probability of binding to their receptors, which then switch from being kinases to being phosphotases, significantly reducing the ratio of [LuxO-P] to [LuxO]. The sRNAs are thus no longer expressed, allowing the synthesis of LuxR and the expression of bioluminescence, for example. Both the phosphorylation-dephosphorylation cascades and the sRNA regulatory network provide a basis for a sharp, sigmoidal response of the concentration of LuxR to smooth changes in cell density.

A. Single-cell model

We will analyze the occurrence of ultrasensitivity in the above quorum sensing system by focusing on a single phosphorylation pathway and adapting the Goldbeter-Koshland of phosphorylation-dephosphorylation cycles (PdPCs) [23]. (For a corresponding model of switching due to the action of sRNAs see Hunter et al. [31]. In their model, the fraction of phosphorylated LuxO is taken to be the external input to the sRNA network. The latter itself depends on the level of phosphorylated LuxU, which is the output of our model. Note that we could also consider ultrasensitivity in a bicyclic PdPC cascade involving both LuxU and LuxO.) In particular, we consider the phosphorylation-dephosphorylation of LuxU by the enzymatic action of a particular quorum sensing receptor, which is denoted by R when acting as a kinase and by $\widehat{R}$ when it is it is bound by an autoinducer (A) and acts like a phosphotase. Denoting the protein LuxU by W, we define the following reaction schemes:

$$W + R \underset{d_1}{\overset{a_1}{\rightleftharpoons}} WR \overset{k_1}{\to} W^* + R \tag{3.1a}$$

$$W^* + \widehat{R} \underset{d_2}{\overset{a_2}{\rightleftharpoons}} W^*\widehat{R} \overset{k_2}{\to} W + \widehat{R}, \tag{3.1b}$$

$$R + A \underset{k_-}{\overset{k_+}{\rightleftharpoons}} \widehat{R}. \tag{3.1c}$$

For simplicity, we assume that both the phosphorylation and the dephosphorylation steps are irreversible. (See the work of Qian and collaborators for an analysis of more detailed, reversible models of PdPCs [25–27].) Introducing the concentrations $u = [A]$, $w = [W]$, $w^* = [W^*]$,

$r = [R]$, $\widehat{r} = [\widehat{R}]$, $v = [WR]$ and $v^* = [W^*\widehat{R}]$, the corresponding kinetic equations for a single cell with a fixed intracellular concentration of autoinducer, are

$$\frac{dw}{dt} = -a_1 w(r - v) + d_1 v + k_2 v^* \tag{3.2a}$$
$$\frac{dv}{dt} = a_1 w(r - v) - (d_1 + k_1)v \tag{3.2b}$$
$$\frac{dw^*}{dt} = -a_2 w^*(\widehat{r} - v^*) + d_2 v^* + k_1 v \tag{3.2c}$$
$$\frac{dv^*}{dt} = a_2 w^*(\widehat{r} - v^*) - (d_2 + k_2)v^* \tag{3.2d}$$
$$\frac{dr}{dt} = k_- \widehat{r} - k_+ u r. \tag{3.2e}$$

These are supplemented by the conservation Eqs.

$$W_T = w + w^* + v + v^*, \tag{3.3a}$$
$$R_T = r + \widehat{r}, \tag{3.3b}$$

where R_T is the total concentration of receptors and W_T is the total concentration of LuxU.

In the various models considered in this paper, the conversion of the receptors from kinase to phosphotase activity is taken to be independent of the PdPC. That is, we ignore any positive feedback pathways, in which the regulation of gene expression by the phosphorylation/dephsophorylation of LuxU alters the production of the autoinducer [32]. This allows us to treat the receptor-ligand dynamics given by Eq. (3.2e), or subsequent extensions, independently of the PdPC dynamics given by Eqs. (3.2a-d). In particular, for fixed concentration u, we can take the concentration of kinases and phosphotases to be at equilibrium:

$$r_{\rm eq} = \frac{k_-}{k_+ u + k_-} R_T \equiv R(u), \quad \widehat{r}_{\rm eq} = R_T - R(u). \tag{3.4}$$

The system of Eqs. (3.2) then reduces to the classical Goldbeter-Koshland model of PdPCs [23], and we can apply their analysis based on a generalization of Michaelis-Menten kinetics. The first step is to assume that the concentration of W and W^* is much larger than that of the receptor, that is, $W_T \gg R_T$ or equivalently $W_T = w + w^*$. This implies that the time scale for the dynamics of the complexes WR and $W^*\widehat{R}$ is much faster than that for the dynamics of W and W^*. Performing a separation of time-scales, we can treat the concentrations w and w^* as constants when analyzing Eqs. (3.2b,d), while we can take the steady-state values of the concentrations v, v^* when solving Eqs. (3.2a,c). Hence, setting $dv/dt = 0$ and $r = R(u)$ in (3.2b) we can solve for v in terms of w. Similarly, setting $dv^*/dt = 0$ and $\widehat{r} = R_T - R(u)$ in (3.2d) we can solve for v^* in terms of w^*. We thus obtain the reduced kinetic scheme

$$W \underset{f_2(w^*)}{\overset{f_1(w)}{\rightleftharpoons}} W^*, \tag{3.5}$$

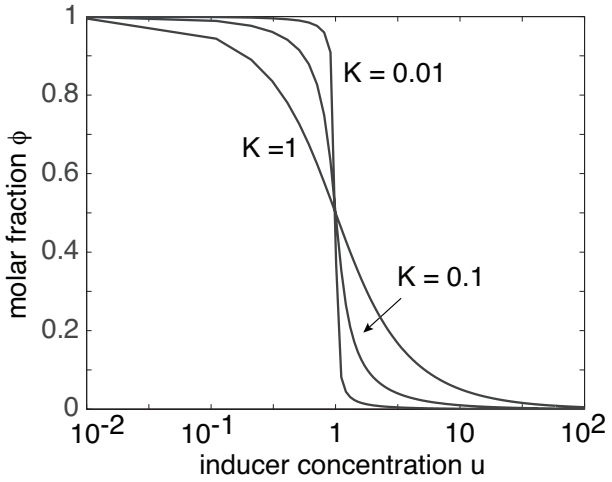

FIG. 3. Molar fraction of modified protein W^* at steady-state as a function of the autoinducer concentration u for different values of K, with $K = K_1 = K_2$ and $k_- k_1 = k_+ k_2$.

with

$$f_1(w) = \frac{k_1 R(u) w}{K_1 + w}, \quad f_2(w^*) = \frac{k_2 [R_T - R(u)] w^*}{K_2 + w^*}, \tag{3.6}$$

and

$$K_1 = \frac{d_1 + k_1}{a_1}, \; K_2 = \frac{d_2 + k_2}{a_2}.$$

Imposing the conservation condition $W_T = w + w^*$ thus yields the single independent kinetic equation

$$\frac{dw^*}{dt} = f_1(W_T - w^*) - f_2(w^*). \tag{3.7}$$

The steady-state concentration $w^*_{\rm eq}$ of LuxU-P is thus obtained by solving $f_1(W_T - w^*) = f_2(w^*)$, which yields a quadratic equation for w^*. Taking the positive root, and expressing it as a function of the fixed autoinducer concentration u, we find that

$$\frac{[\text{LuxU-P}]}{[\text{LuxU-P}]+[\text{LuxU}]} = \phi(V(u)), \tag{3.8}$$

with

$$V(u) = \frac{k_1 R(u)}{k_2 [R_T - R(u)]} = \frac{k_-}{k_+ u} \frac{k_1}{k_2} \tag{3.9}$$

and ϕ given by

$$\phi = \frac{-B + \sqrt{B^2 + 4AC}}{2AW_T}, \tag{3.10}$$

for $V \neq 1$, where

$$A = V(u) - 1, \quad B = \frac{1}{W_T}\left(K_1 + K_2 V(u)\right) - \left(V(u) - 1\right),$$
$$C = \frac{K_2}{W_T} V(u).$$

A plot of ϕ, as a function of the autoinducer concentration u is shown in Fig. 3 for $K_1 = K_2 = K$. At low values of K, there is a sharp change from high to low levels of modified protein over a very small change in u (ultrasensitivity); this corresponds to a regime in which the two enzymes are saturated. On the other hand, for large values of K, the curve is relatively shallow, and one obtains a response similar to first-order kinetics.

Note on units

In this paper we are concerned with certain qualitative features of the quorum sensing network. Therefore, we treat all parameters and variables as dimensionless. We fix the units of autoinducer concentration by taking the PdPC switch to occur at $u = 1$. (Typical intracellular molar concentrations are of order nM.) The receptor concentration r is expressed in terms of the fraction of receptors that act as kinases by setting $R_T = 1$. Similarly, the concentration of LuxU-R is expressed in terms of the fraction of phosphorylated LuxU proteins by setting $W_T = 1$. Finally, the units of time are taken to be of the order minutes, comparable to typical unbinding times k_-^{-1}. In all figures variables are dimensionless.

B. Global convergence of population model

Now consider a population of N identical cells that are coupled via a common extracellular domain due to the transfer of the autoinducer A across the cell membrane. Eq. (3.2e) for a single cell is then replaced by a system of equations of the form (2.1),

$$\frac{du_i}{dt} = \Gamma + k_-(R_T - r_i) - k_+ u_i r_i - \kappa(u_i - U), \quad (3.11a)$$

$$\frac{dr_i}{dt} = k_-(R_T - r_i) - k_+ u_i r_i \quad i = 1, \ldots, N \quad (3.11b)$$

$$\frac{dU}{dt} = \alpha\kappa(u_{\rm av} - U) - \gamma U, \quad (3.11c)$$

where

$$u_{\rm av} = \frac{1}{N}\sum_{j=1}^{N} u_j, \quad (3.12)$$

is the population-averaged intracellular concentration of A, U is the extracellular concentration of A, and Γ is the rate of production of A due to the action of enzymes.

We would like to use contraction analysis (section II) to derive conditions that ensure global convergence of the system (3.11). In order to achieve this, it is first necessary to obtain an upper bound on u_i for any i. (Since u_i is a concentration, the lower bound is given by $u_i \geq 0$.) Eq. (3.11c) implies that

$$U(t) \leq \frac{\alpha\kappa u_{\rm av}(t)}{\alpha\kappa + \gamma},$$

with $u_{\rm av}(t)$ evolving according to

$$\frac{du_{\rm av}}{dt} = \Gamma + \frac{k_-}{N}\sum_{i=1}^{N}(R_T - r_i) - \frac{k_+}{N}\sum_{i=1}^{N}(u_i r_i) - \kappa(u_{\rm av} - U).$$

The latter is obtained by summing Eq. (3.11a) with respect to i. It follows that

$$\frac{du_{\rm av}}{dt} \leq \Gamma + k_- R_T - \kappa(u_{\rm av} - U) \leq \Gamma + k_- R_T - \frac{\kappa\gamma}{\alpha\kappa + \gamma} u_{\rm av},$$

Hence, using a comparison principle, if $u_{\rm av}(0) \leq v(0)$ then $u_{\rm av}(t) \leq v(t)$ for all $t > 0$ with

$$\frac{dv}{dt} = \Gamma + k_- R_T - \frac{\kappa\gamma}{\alpha\kappa + \gamma} v,$$

Moreover, if

$$v(0) \leq \Theta \equiv \frac{(\Gamma + k_- R_T)(\alpha\kappa + \gamma)}{\kappa\gamma},$$

then $v(t) \leq \Theta$ for all $t > 0$ and thus

$$u_{\rm av}(t) \leq \Theta, \quad \text{for all } t > 0.$$

This in turn means that

$$U(t) \leq \frac{\alpha}{\gamma}(\Gamma + k_- R_T),$$

which leads to an upper bound on each $u_i(t)$:

$$u_i(t) \leq \Theta. \quad (3.13)$$

Let us now consider global convergence of Eqs. (3.11). The reduced virtual system takes the form

$$\frac{dy_1}{dt} = \Gamma + k_-[R_T - y_2] - k_+ y_1 y_2 - \kappa(y_1 - U), \quad (3.14a)$$

$$\frac{dy_2}{dt} = k_-[R_T - y_2] - k_+ y_1 y_2, \quad (3.14b)$$

with $U(t)$ treated as an external input. The Jacobian of the virtual system is

$$J(\mathbf{y}, t) = \begin{pmatrix} -k_+ y_2 - \kappa & -k_- - k_+ y_1 \\ -k_+ y_2 & -k_- - k_+ y_1 \end{pmatrix}. \quad (3.15)$$

Suppose that we take the ℓ_2 norm for $\mathbf{y}$. In order to determine the corresponding matrix measure $\mu_2(J)$, we need to calculate the eigenvalues of the symmetric matrix

$$\frac{J + J^*}{2} = \begin{pmatrix} -k_+ y_2 - \kappa & -[k_- + k_+(y_1 + y_2)]/2 \\ -[k_- + k_+(y_1 + y_2)]/2 & -k_- - k_+ y_1 \end{pmatrix}.$$

These are given by

$$\lambda_\pm = \frac{1}{2}\left[-b(\mathbf{y}) \pm \sqrt{b(\mathbf{y})^2 - c(\mathbf{y})}\right],$$

with

$$b(\mathbf{y}) = \kappa + k_- + k_+(y_1 + y_2)$$
$$c(\mathbf{y}) = 4(\kappa + k_+ y_2)(k_- + k_+ y_1) - [k_- + k_+(y_1 + y_2)]^2.$$

Since $b(\mathbf{y}) > 0$, the matrix measure is

$$\mu_2(J) = \max\{\lambda_\pm\} = \lambda_+.$$

Hence, the virtual system is contracting provided that $c(\mathbf{y}) > 0$.

We now derive conditions for $c(\mathbf{y})$ to be positive definite. First, note that

$$c(0) = k_-(4\kappa - k_-) > 0$$

provided $\kappa > k_-/4$. Assuming this inequality holds, we can ensure positivity of $c(\mathbf{y})$ by imposing the following conditions:

$$\frac{\partial c}{\partial y_1} \equiv 2k_+[2\kappa - 2k_- - k_+(y_1 - y_2)] > 0,$$
$$\frac{\partial c}{\partial y_2} \equiv 2k_+[k_- + k_+(y_1 - y_2)] > 0.$$

for all $\mathbf{y}$. The minimum possible value of $\partial_2 c$ occurs when $y_2 = R_T$ and $y_1 = 0$, which will be positive definite provided

$$k_+ R_T < k_- < 4\kappa. \tag{3.16}$$

The minimum possible value of $\partial_1 c$ occurs when $y_1 = \Theta$, see Eq. (3.13), which will be positive definite provided

$$k_- + k_+\Theta < 2\kappa. \tag{3.17}$$

We have thus proven that if conditions (3.16) and (3.17) hold, then $\mu_2(J) < 0$ and the $\mathbf{y}$ dynamics is contracting. Applying the notion of partial contraction, we thus deduce that the quorum sensing system (3.11) is globally convergent with $u_i(t) \to u(t)$ and $r_i(t) \to r(t)$ in the limit $t \to \infty$, with (u, r) evolving according to the effective single-cell model

$$\frac{du}{dt} = \Gamma + k_-[R_T - r] - k_+ ur - \kappa(u - U) \tag{3.18a}$$
$$\frac{dr}{dt} = k_-[R_T - r] - k_+ ur \tag{3.18b}$$
$$\frac{dU}{dt} = \alpha\kappa(u - U) - \gamma U, \tag{3.18c}$$

An illustration of global convergence is presented in Fig. 4, where we plot the evolution of the inducer concentration for 10 coupled cells based on numerically solving Eqs. (3.11).

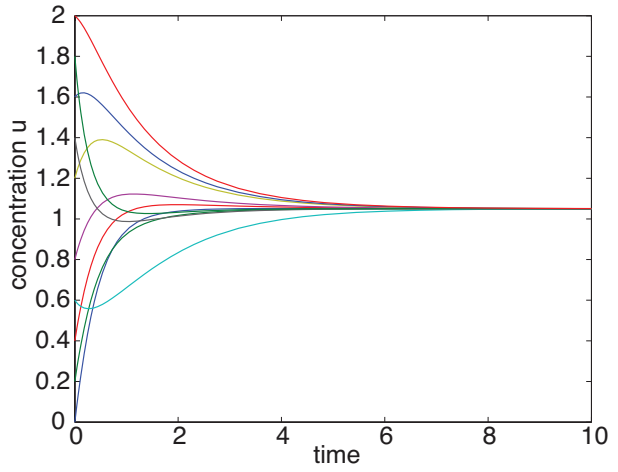

FIG. 4. (Color online) Global convergence of the intracellular autoinducer concentration for $N = 10$ coupled cells. Parameter values are $k_- = k_+ = \Gamma = 1$, $R_T = 1$, $\kappa = 1$, and $\alpha = 0.05$.

C. Ultrasensitivity in population model

Global convergence of the quorum sensing system means that, ignoring transients, we can explore the effects of the extracellular coupling on ultrasensitivity of the PdPC pathway by taking the cells to be synchronized and evolving according to Eqs. (3.18). The latter have a unique stable fixed point $u_{\rm eq}$ with

$$u_{\rm eq} = \Gamma\frac{(\alpha\kappa + \gamma)}{\kappa\gamma} \equiv \psi(\alpha). \tag{3.19}$$

Putting $u = u_{\rm eq}$ in Eq. (3.8) finally shows that

$$\frac{[\text{LuxU-P}]}{[\text{LuxU-P}]+[\text{LuxU}]} = \phi\left(\frac{k_-}{k_+\psi(\alpha)}\frac{k_1}{k_2}\right) \equiv \Psi(\alpha), \tag{3.20}$$

In order that the system exhibit switch-like behavior as a function of cell density α, we require a critical value α_c, $0 < \alpha_c < \infty$ such that (for $\Gamma = 1$)

$$\chi \equiv \frac{k_-}{k_+}\frac{k_1}{k_2} = \frac{\alpha_c}{\gamma} + \frac{1}{\kappa},$$

that is

$$\alpha_c = \gamma(\chi - \kappa^{-1}).$$

Assuming that $\chi = 1$ and taking $\alpha_c = 0.05$ [14], we require $\kappa > 1$ and $\gamma = \gamma_c = 0.05(1 - \kappa^{-1})$. For low cell densities ($\alpha \ll \alpha_c$) we have $\Psi(\alpha) \approx 1$, which follows from the functional form of ϕ, see Fig. 3. Hence the fraction of phosphorylated LuxU-P is high, which ultimately means that the expression of the gene regulator protein LuxR is suppressed. On the other hand, for large cell densities ($\alpha \gg \alpha_c$) we find that $\Psi(\alpha) \approx 0$. Now the fraction of phosphorylated LuxU-P is small, allowing the expression of LuxR and downstream gene regulatory networks. The α-dependence is illustrated in Fig. 5. Since, α and u are lineraly related, we will focus on the u-dependence in subsequent sections and choose γ and Γ such that $\alpha_c = 0.05$ for all κ.

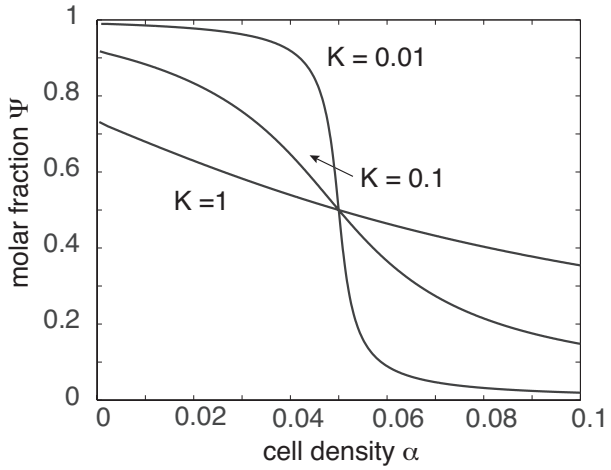

FIG. 5. Molar fraction of modified protein W^* at steady-state as a function of the cell density α for different values of K, $K = K_1 = K_2$. Other parameter values are chosen so that $k_- k_1 = k_+ k_2$, $\Gamma = 1$, $\kappa = 10$, $\alpha_c = 0.05$.

IV. NOISE AMPLIFICATION OF INTRINSIC FLUCTUATIONS

One of the characteristic features of ultrasensitive biochemical signaling networks is that they tend to amplify noise [24, 26, 33, 34]. On the other hand, collective behavior at the population level, as exhibited by quorum sensing networks, can mitigate the effects of noise [28, 35]. In this section we explore the amplification of intrinsic fluctuations in the *V. harveyi* quorum sensing model introduced in Sec. III. Note that our analysis is distinct from some recent studies based on stochastic versions of Eqs. (2.1), in which the mass-action kinetics of the auxiliary species within each cell is replaced by a master equation describing the stochastic reactions of a finite number of molecules [36, 37]. We will assume throughout that the population model is contracting as defined in Sect. II.

A. Linear response of single-cell model

We begin by returning to the single cell model with fixed concentration u of autoinducer. In the deterministic case, with r given by the equilibrium solution (3.4), the dynamics of LuxU is given by equation (3.7), which we write explicitly in the form

$$\frac{dw^*}{dt} = \mathcal{F}(w^*, r) \equiv \frac{k_1 r(W_T - w^*)}{K_1 + [W_T - w^*]} - \frac{k_2[R_T - r]w^*}{K_2 + w^*}. \tag{4.1}$$

A number of recent studies have investigated noise signal amplification in ultrasensitive signal transduction based on stochastic versions of Eq. (4.1) [24, 26, 33, 34]. A more detailed analysis would need to start from a stochastic version of the full system of Eqs. (3.2), since $r(t)$ is now time-dependent. Here, however, we will follow along similar lines to previous authors and consider the effects of fluctuations in receptor concentration by applying linear response theory to Eq. (4.1).

Suppose that $r(t)$ undergoes small fluctuations about the equilibrium state $r_{\rm eq}$ of Eq. (3.4). This can be incorporated by replacing Eq. (3.2) for fixed u by the Langevin equation

$$\frac{dr}{dt} = k_-(R_T - r) - k_+ ur + \sigma_0 \xi(t), \tag{4.2}$$

with $\xi(t)$ a white noise process,

$$\langle \xi(t) \rangle = 0, \quad \langle \xi(t)\xi(t') \rangle = \delta(t - t'),$$

and σ_0 a fixed noise intensity. One possible source of noise is fluctuations in the autoinducer concentration u; these will be modeled explicitly in the population model of quorum sensing in Sec. IIIB. Under the linear noise approximation, we set $r(t) = r_{\rm eq} + R(t)$ such that

$$\frac{dR}{dt} = -(k_- + k_+ u)R + \sigma_0 \xi(t). \tag{4.3}$$

Similarly, linearizing equation (4.1) about the equilibrium solution by setting $w^* = w^*_{\rm eq} + W$, $w^*_{\rm eq} = \phi(V(u))$, gives

$$\frac{dW}{dt} = -\beta_1 W + \beta_2 R, \tag{4.4}$$

with

$$\beta_1 = -\left.\frac{\partial \mathcal{F}}{\partial w^*}\right|_{\rm eq} = \frac{k_1 K_1 r_{\rm eq}}{[K_1 + [W_T - w^*_{\rm eq}]]^2} + \frac{k_2 K_2 [R_T - r_{\rm eq}]}{[K_2 + w^*_{\rm eq}]^2} \tag{4.5}$$

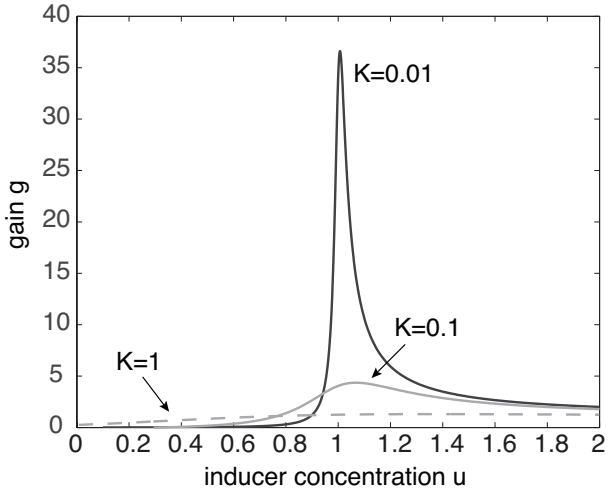

FIG. 6. Plot of deterministic gain g of single-cell model as a function of autoinducer concentration u for different values of K, $K = K_1 = K_2$. Other parameter values are $k_- = k_+ = k_1 = k_2 = 1$, and $R_T = W_T = 1$.

and

$$\beta_2 = \left.\frac{\partial \mathcal{F}}{\partial r}\right|_{\rm eq} = \frac{k_1(W_T - w^*_{\rm eq})}{K_1 + [W_T - w^*_{\rm eq}]} + \frac{k_2 w^*_{\rm eq}}{K_2 + w^*_{\rm eq}} \qquad (4.6)$$

Note that the gain of the underlying deterministic system (4.1) at equilibrium is given by

$$g = \frac{\Delta W/w^*_{\rm eq}}{\Delta R/r_{\rm eq}} = \frac{\beta_2}{\beta_1}\frac{r_{\rm eq}}{w^*_{\rm eq}}. \qquad (4.7)$$

Incorporating the u-dependence of $r_{\rm eq}$ and $\beta_{1,2}$ we determine $g = g(u)$. In Fig. 6 we plot the gain g as a function of u. It can be seen that there is a sharp gain around the critical concentration $u = 1$.

In order to determine the variance of the concentration of LuxU-P, w^*, we use Fourier transforms. Taking

$$R(\omega) = \int_{-\infty}^{\infty} {\rm e}^{i\omega t} R(t) dt$$

etc., we Fourier transform the linear equations (4.3) and (4.4) to obtain

$$W(\omega) = \frac{\beta_2}{\beta_1 + i\omega} R(\omega), \quad R(\omega) = \frac{\sigma_0}{k_- + k_+ u + i\omega}\xi(\omega),$$

where $\xi(\omega)$ is the Fourier transform of a white noise process with

$$\langle \xi(\omega)\rangle = 0, \quad \langle \xi(\omega)\overline{\xi(\omega')}\rangle = 2\pi\delta(\omega - \omega').$$

Using the Wiener-Khinchine theorem, the variance of the receptor concentration is given by the integral of the power spectrum defined by

$$2\pi S_R(\omega)\delta(\omega - \omega') = \langle R(\omega)\overline{R(\omega')}\rangle$$

That is,

$$\begin{aligned}\sigma_R^2 &= \int_{-\infty}^{\infty} S_R(\omega)\frac{d\omega}{2\pi} \\ &= \int_{-\infty}^{\infty} \frac{\sigma_0^2}{[k_- + k_+ u]^2 + \omega^2}\frac{d\omega}{2\pi} \\ &= \frac{\sigma_0^2}{2[k_- + k_+ u]}. \end{aligned} \qquad (4.8)$$

Similarly, the variance of the Lux-P concentration is

$$\begin{aligned}\sigma_W^2 &= \int_{-\infty}^{\infty} S_W(\omega)\frac{d\omega}{2\pi} \\ &= \int_{-\infty}^{\infty} \frac{\beta_2^2}{\beta_1^2 + \omega^2}\frac{\sigma_0^2}{[k_- + k_+ u]^2 + \omega^2}\frac{d\omega}{2\pi} \\ &= \frac{\beta_2^2}{\beta_1^2 - [k_- + k_+ u]^2}\frac{\sigma_0^2}{2[k_- + k_+ u]} \\ &\quad + \frac{\beta_2^2}{2\beta_1}\frac{\sigma_0^2}{[k_- + k_+ u]^2 - \beta_1^2} \\ &= \frac{\beta_2^2\sigma_0^2}{2\beta_1[k_- + k_+ u]}\frac{1}{k_- + k_+ u + \beta_1}. \end{aligned} \qquad (4.9)$$

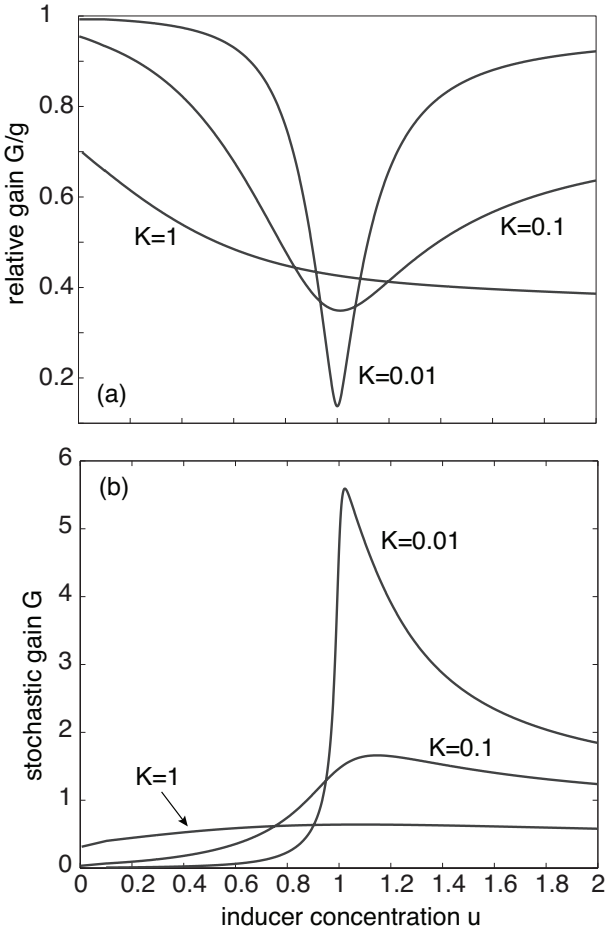

FIG. 7. Plot of (a) relative gain G/g and (b) stochastic gain G as a function of autoinducer concentration u for different values of K, $K = K_1 = K_2$. Other parameter values are $k_- = k_+ = k_1 = k_2 = 1$, and $R_T = W_T = 1$.

If we interpret $\sigma_W/w^*_{\rm eq}$ as the relative noise intensity of the output and $\sigma_R/r_{\rm eq}$ as the relative noise intensity of the output, then the noise amplification of the PdPC in response to receptor fluctuations is defined by the stochastic gain [33]

$$\begin{aligned} G &= \frac{\sigma_W/w^*_{\rm eq}}{\sigma_R/r_{\rm eq}} = \frac{r_{\rm eq}}{w^*_{\rm eq}}\sqrt{\frac{\beta_2^2}{\beta_1}\frac{1}{k_- + k_+ u + \beta_1}} \\ &= g\sqrt{\frac{\beta_1}{k_- + k_+ u + \beta_1}}, \end{aligned} \qquad (4.10)$$

where g is the deterministic gain (4.7). In Fig. 7 we plot the relative gain G/g and the stochastic gain G as a function of u. It can be seen that the sharp amplification around the critical density $u = 1$ in the ultrasensitive regime ($K = 0.01$) is suppressed relative to the deterministic gain.

B. Linear response of population model

We now extend the analysis of noise amplification to the population model, where we explicitly model the stochastic dynamics of the autodinducer concentration. We show how filtering of the noise by the quorum sensing network can greatly reduce the effects of noise amplification. The first point to note is that in a stochastic model of quorum sensing, we cannot identify the state of all the cells, even if the deterministic system (2.1) is globally convergent. Therefore, in the case of *V. harveyi*, we have to consider a stochastic version of Eqs. (3.11a,b):

$$\frac{du_i}{dt} = \Gamma + k_-(R_T - r_i) - k_+ u_i r_i - \kappa(u_i - U) + \theta_0 \xi_i(t), \tag{4.11a}$$

$$\frac{dr_i}{dt} = k_-(R_T - r_i) - k_+ u_i r_i, \tag{4.11b}$$

$$\frac{dU}{dt} = \alpha\kappa(u_{\rm av} - U) - \gamma U \tag{4.11c}$$

for $i = 1, \ldots, N$, with

$$\langle \xi_i(t) \rangle = 0, \quad \langle \xi_i(t) \xi_j(t') \rangle = \delta(t - t') \delta_{ij}.$$

We assume that each cell is driven by an independent white noise term with constant noise intensity θ_0; one source of the noise could be fluctuations in the production of the autoinducer. Linearizing about the global steady-state by setting

$$u_i(t) = u_{\rm eq} + \mathcal{U}_i(t),\ r_i(t) = r_{\rm eq} + R_i(t),\ U(t) = U_{\rm eq} + \mathcal{V}(t),$$

yields

$$\frac{d\mathcal{U}_i}{dt} = -k_- R_i - k_+(\mathcal{U}_i r_{\rm eq} + u_{\rm eq} R_i) - \kappa(\mathcal{U}_i - \mathcal{V}) + \theta_0 \xi_i(t), \tag{4.12a}$$

$$\frac{dR_i}{dt} = -k_- R_i - k_+(\mathcal{U}_i r_{\rm eq} + u_{\rm eq} R_i), \tag{4.12b}$$

$$\frac{d\mathcal{V}}{dt} = \alpha\kappa(\mathcal{U}_{\rm av} - \mathcal{V}) - \gamma \mathcal{V}, \quad \mathcal{U}_{\rm av} = \frac{1}{N} \sum_{i=1}^{N} \mathcal{U}_i. \tag{4.12c}$$

Fourier transforming this linear system of equations gives

$$\Gamma_U(\omega) \mathcal{U}_i(\omega) = -(k_- + k_+ u_{\rm eq}) R_i(\omega) + \kappa \mathcal{V}(\omega) + \theta_0 \xi_i(\omega), \tag{4.13a}$$

$$\Gamma_R(\omega) \mathcal{R}_i(\omega) = -k_+ r_{\rm eq} \mathcal{U}_i(\omega), \tag{4.13b}$$

$$\Gamma_V(\omega) \mathcal{V}(\omega) = \alpha\kappa \mathcal{U}_{\rm av}(\omega). \tag{4.13c}$$

where

$$\Gamma_U(\omega) = i\omega + \kappa + k_+ r_{\rm eq}, \quad \Gamma_R(\omega) = i\omega + k_- + k_+ u_{\rm eq},$$
$$\Gamma_V(\omega) = i\omega + \gamma + \alpha\kappa.$$

Summing both sides of Eqs. (4.13a,b) with respect to i and using Eq. (4.13c) we obtain the result

$$R_{\rm av}(\omega) = -\frac{k_+ r_{\rm eq} \mathcal{U}_{\rm av}(\omega)}{\Gamma_R(\omega)}, \quad \mathcal{U}_{\rm av}(\omega) = \frac{\theta_0 \xi_{\rm av}(\omega)}{\widehat{\Gamma}_U(\omega)}, \tag{4.14}$$

where

$$\widehat{\Gamma}_U(\omega) = \Gamma_U(\omega) - \frac{k_+ r_{\rm eq}(k_- + k_+ u_{\rm eq})}{\Gamma_R(\omega)} - \frac{\alpha\kappa^2}{\Gamma_V(\omega)}.$$

It follows that

$$\left(\widehat{\Gamma}_U(\omega) + \Lambda(\omega)\right) U_i(\omega) = \theta_0 \xi_i(\omega) + \Lambda(\omega) \mathcal{U}_{\rm av}(\omega), \tag{4.15}$$

where

$$\Lambda(\omega) = \frac{\alpha\kappa^2}{\Gamma_V(\omega)}.$$

Multiplying Eq. (4.15) by its complex conjugate and averaging with respect to the noise gives

$$(\widehat{\Gamma}_U(\omega) + \Lambda(\omega))\overline{(\widehat{\Gamma}_U(\omega') + \Lambda(\omega'))} \langle U_i(\omega) \overline{U_i(\omega')} \rangle = \theta_0^2 \langle \xi_i(\omega) \overline{\xi_i(\omega')} \rangle + \Lambda(\omega) \overline{\Lambda(\omega')} \langle \mathcal{U}_{\rm av}(\omega) \overline{\mathcal{U}_{\rm av}(\omega')} \rangle + \theta_0 \overline{\Lambda(\omega')} \langle \xi_i(\omega) \overline{\mathcal{U}_{\rm av}(\omega')} \rangle + \Lambda(\omega) \langle \mathcal{U}_{\rm av}(\omega) \overline{\xi_i(\omega')} \rangle.$$

From Eq. (4.14), we find that

$$\langle \mathcal{U}_{\rm av}(\omega) \overline{\mathcal{U}_{\rm av}(\omega')} \rangle = \frac{2\pi\theta_0^2}{N|\widehat{\Gamma}_U(\omega)|^2} \delta(\omega - \omega'),$$
$$\langle \xi_i(\omega) \overline{\mathcal{U}_{\rm av}(\omega')} \rangle = \frac{2\pi\theta_0}{N\overline{\widehat{\Gamma}_U(\omega)}} \delta(\omega - \omega').$$

Each cell thus has the same spectrum S_U with

$$S_U(\omega) = \frac{\theta_0^2}{|\widehat{\Gamma}_U(\omega) + \Lambda(\omega)|^2} \times \left(1 + \frac{|\Lambda(\omega)|^2}{N|\widehat{\Gamma}_U(\omega)|^2} + \frac{2}{N} {\rm Re}\left[\frac{\Lambda(\omega)}{\widehat{\Gamma}_U(\omega)}\right]\right) \tag{4.16}$$

Now suppose that N is sufficiently large so that the

$O(1/N)$ terms can be dropped. The remaining denominator can be simplified by noting that

$$\widehat{\Gamma}_U(\omega)+\Lambda(\omega)=i\omega+\kappa+k_+r_{\rm eq}-\frac{k_+r_{\rm eq}(k_-+k_+u_{\rm eq})}{i\omega+k_-+k_+u_{\rm eq}}=\frac{(i\omega+z_+)(i\omega+z_-)}{i\omega+k_-+k_+u_{\rm eq}},$$

with

$$z_\pm=\frac{1}{2}\left[(k_-+k_+(u_{\rm eq}+r_{\rm eq})+\kappa)\pm\sqrt{(k_-+k_+(u_{\rm eq}+r_{\rm eq})+\kappa)^2-4\kappa(k_-+k_+u_{\rm eq})}\right].$$

Noting that $z_\pm$ are real with $z_\pm>0$, we see that the denominator of $S_U(\omega)$ has simple poles at $w=-iz_-\pm$ and $w=iz_\pm$ with $iz_\pm$ lying in the upper-half complex plane. Hence, using Eq. (4.13b), the variance in the receptor concentration r_i at the single cell level is (after closing the contour C in the upper-half plane)

$$\sigma_R^2=\frac{(k_+r_{\rm eq})^2}{|\Gamma_R(\omega)|^2}\int_{-\infty}^{\infty}S_U(\omega)\frac{d\omega}{2\pi}=\oint_C\frac{\sigma_0^2}{|i\omega+z_+|^2|i\omega+z_-|^2}\frac{d\omega}{2\pi}=\frac{\sigma_0^2}{2z_-(z_+^2-z_-^2)}-\frac{\sigma_0^2}{2z_+(z_+^2-z_-^2)}=\frac{\sigma_0^2}{2z_+z_-(z_++z_-)},\tag{4.17}$$

where we have taken $\sigma_0=k_+r_{\rm eq}\theta_0/\Gamma$ with $\Gamma=1$. It is straightforward to show that $\sigma_R^2\to 0$ as $\kappa\to\infty$. This is illustrated in Fig. 8, where we plot the ratio σ_R^2/σ_0^2 as a function of $u_{\rm eq}$ for various κ. Hence, the receptor fluctuations vanish in the limit $N,\kappa\to\infty$, which is consistent with the nonlinear analysis of Sec. IVC.

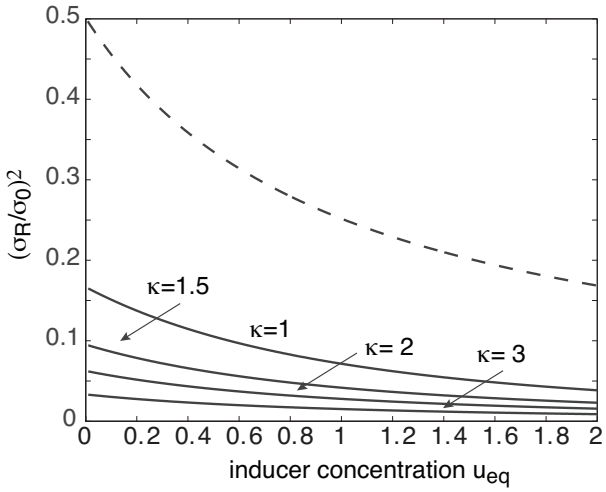

FIG. 8. Plot of variance σ_R^2 in receptor fluctuation G as a function of autoinducer concentration $u_{\rm eq}$ for different values of κ. Other parameter values are $k_-=k_+=k_1=k_2=1$, and $R_T=W_T=1$. Also shown is the corresponding quantity in the single-cell model (dashed curve).

We now calculate the gain of individual cell PdPCs driven by the receptor fluctuations of the population model. Following along identical lines to Sec. IIIB,

$$\begin{aligned}\sigma_W^2&=\int_{-\infty}^{\infty}S_W(\omega)\frac{d\omega}{2\pi}\\&=\int_{-\infty}^{\infty}\frac{\beta_2^2}{\beta_1^2+\omega^2}\frac{\sigma_0^2}{|i\omega+z_+|^2|i\omega+z_-|^2}\frac{d\omega}{2\pi}\\&=\frac{\beta_2^2}{2\beta_1^2}\frac{\beta_1^2\sigma_0^2}{(\beta_1^2-z_+^2)(\beta_1^2-z_-^2)}\\&\quad\times\left[\frac{\beta_1^2-(z_-^2+z_-z_++z_+^2)}{(z_++z_-)z_+z_-}+\frac{1}{\beta_1}\right].\end{aligned}\tag{4.18}$$

The gain G is then

$$\begin{aligned}G&=\frac{\sigma_W/w_{\rm eq}^*}{\sigma_R/r_{\rm eq}}=g\frac{\beta_1\sigma_W}{\beta_2\sigma_R},\\&=g\sqrt{\frac{\beta_1}{(\beta_1^2-z_+^2)(\beta_1^2-z_-^2)}}\\&\quad\times\sqrt{\beta_1[\beta_1^2-(z_-^2+z_-z_++z_+^2)]+(z_++z_-)z_+z_-}.\end{aligned}\tag{4.19}$$

Expressing $r_{\rm eq}$ and $\beta_{1,2}$ in terms of $u_{\rm eq}$, we plot the stochastic gain G of the population model as a function of $u_{\rm eq}$ for $K=0.01$ and various coupling strengths κ, see Fig. 9. We find that the stochastic gain G is only weakly dependent on κ, and approaches the gain of the single-cell model as κ increases. Given that the receptor fluctuations σ_R^2 are suppressed in the quorum sensing model for large κ, while the gain is hardly changed, we conclude that the fluctuations in the LuxU-P concentration w^* are greatly suppressed compared to an isolated cell.

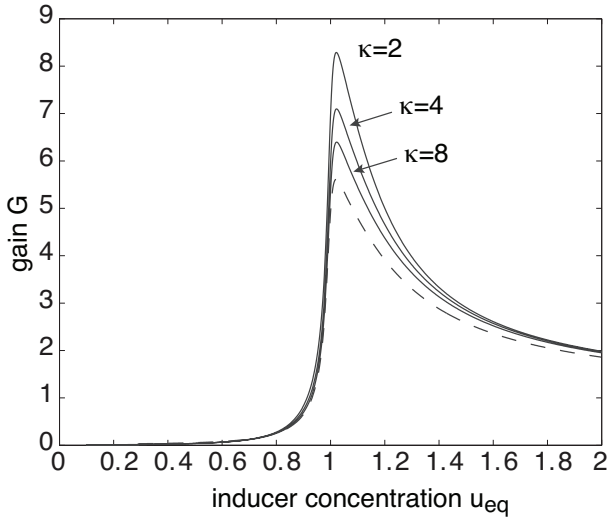

FIG. 9. Plot of stochastic gain G of population model as a function of autoinducer concentration $u_{\rm eq}$ for different values of κ and $K = 0.01$. Other parameter values are $k_- = k_+ = k_1 = k_2 = 1$, and $R_T = W_T = 1$. Dashed curve is gain of single-cell model from Fig. 7(b).

C. Nonlinear stochastic analysis

In Sec. IVB we showed that within the framework of linear response theory, the variance in receptor fluctuations vanishes in the limit $N \to \infty$ and $\kappa \to \infty$. It turns out that this result also holds for the full nonlinear model, which can be established by applying the contraction analysis of Refs. [28, 35]. First, we rewrite Eqs. (4.11a,b) in the more compact form

$$\frac{d\mathbf{x}_i}{dt} = \mathbf{f}(\mathbf{x}_i) + \mathbf{e}_1\theta_0\xi_i(t), \tag{4.20}$$

with $\mathbf{x} = (u, r)$, $\mathbf{e}_1 = (1, 0)$,

$$f_1(\mathbf{x}) = \Gamma + k_-(R_T - r) - k_+ur - \kappa(u_i - U),$$
$$f_2(\mathbf{x}) = k_-(R_T - r) - k_+ur.$$

Summing both sides of Eq. (4.20) with respect to i and setting $\mathbf{x}_{\rm av} = N^{-1}\sum_{i=1}^N \mathbf{x}_i$, we have

$$\frac{d\mathbf{x}_{\rm av}}{dt} = \mathbf{f}(\mathbf{x}_{\rm av}) + \varepsilon + \mathbf{e}_1\frac{\theta_0}{N}\sum_{i=1}^N \xi_i(t), \tag{4.21}$$

where

$$\varepsilon = \frac{1}{N}\sum_{i=1}^N \mathbf{f}(\mathbf{x}_i) - \mathbf{f}(\mathbf{x}_{\rm av}).$$

In order to estimate $\|\varepsilon\|_2$ we use the Taylor expansion formula with integral remainder:

$$f_k(\mathbf{x}_i) = f_k(\mathbf{x}_{\rm av}) + \int_0^1 \nabla f_k(\mathbf{x}_i(s)) \cdot \frac{d\mathbf{x}_i}{ds} ds$$

where $\mathbf{x}_i(s) = (1 - s)\mathbf{x}_{\rm av} + s\mathbf{x}_i$. Integrating by parts,

$$f_k(\mathbf{x}_i) = f_k(\mathbf{x}_{\rm av}) + (\mathbf{x}_i - \mathbf{x}_{\rm av}) \cdot \nabla f_k(\mathbf{x}_{\rm av}) + \int_0^1 \sum_{l,l'=1,2} (\mathbf{x}_i(s) - \mathbf{x}_{\rm av})_l H_{k,ll'}(\mathbf{x}_i(s))(\mathbf{x}_i(s) - \mathbf{x}_{\rm av})_{l'} ds$$

where $\mathbf{H}$ is the Hessian matrix

$$H_{k,ll'}(\mathbf{x}) = \frac{\partial^2 f_k}{\partial x_l x_{l'}}.$$

We shall assume that for $k = 1, 2$, the largest eigenvalue $\lambda_{\max}(\mathbf{H}_k)$ of the Hessian matrix is uniformly bounded from above by a constant $H_{\rm bd}/\sqrt{2}$. This means in particular that for all $\mathbf{x}$,

$$\mathbf{x} \cdot \mathbf{H}_k\mathbf{x} \le \frac{H_{\rm bd}}{\sqrt{2}}\|\mathbf{x}\|^2.$$

Averaging both sides with respect to i and taking absolute values then implies

$$\left|\frac{1}{N}\sum_{i=1}^N f_k(\mathbf{x}_i) - f_k(\mathbf{x}_{\rm av})\right| \le \frac{H_{\rm bd}}{\sqrt{2}N}\int_0^1 \sum_{i=1}^N \|\mathbf{x}_i(s) - \mathbf{x}_{\rm av}\|^2 ds$$
$$\le \frac{H_{\rm bd}}{2\sqrt{2}N}\sum_{i=1}^N \|\mathbf{x}_i - \mathbf{x}_{\rm av}\|^2.$$

It immediately follows that

$$\|\varepsilon\|_2 \le \frac{H_{\rm bd}}{2N}\sum_{i=1}^N \|\mathbf{x}_i - \mathbf{x}_{\rm av}\|^2.$$

Following Ref. [28, 35], suppose that after a transient

phase,

$$\mathbb{E}\left[\sum_{i=1}^{N}\|\mathbf{x}_i-\mathbf{x}_{\rm av}\|^2\right]=\frac{1}{N}\mathbb{E}\left[\sum_{i<j}^{N}\|\mathbf{x}_i-\mathbf{x}_j\|^2\right]\leq\frac{\rho}{N}. \tag{4.22}$$

This then implies

$$\mathbb{E}[\|\varepsilon\|_2]\leq\frac{H_{\rm bd}}{2N^2}\rho \tag{4.23}$$

for some finite ρ. We find that $\rho\sim N^2/\kappa$ so that $\mathbb{E}[\|\varepsilon\|_2]\to 0$ as $\kappa\to\infty$ Finally, returning to Eq. (4.21), we note that since the noise terms $\xi_i(t)$ are independent,

$$\frac{\sigma}{N}\sum_{i=1}^{N}\xi_i(t)\approx\frac{1}{\sqrt{N}}\xi(t).$$

Hence, in the limit $N,\kappa\to\infty$, the difference between trajectories $\mathbf{x}_{\rm av}(t)$ and those of the deterministic system $\mathbf{y}=\mathbf{f}(\mathbf{y})$ tend to zero, and this then carries over to individual trajectories $\mathbf{x}_i(t)$.

It remains to establish the inequality (4.22). We will adapt the analysis of coupled FitzHugh-Nagumo oscillators presented in Ref. [35]. Let us first consider two cells ($N=2$) with states (u_1,r_1), (u_2,r_2). We construct the following linear virtual system, for which (u_1,r_1,u_2,r_2) are treated as external inputs:

$$\frac{dx_1}{dt}=-k_-x_2-k_+(r_1+r_2)x_1-k_+(u_1+u_2)x_2-\kappa x_1+\theta_0\xi(t) \tag{4.24a}$$

$$\frac{dx_2}{dt}=-k_-x_2-k_+(r_1+r_2)x_1-k_+(u_1+u_2)x_2. \tag{4.24b}$$

Comparison with Eqs. (4.20) for $i=1,2$ implies that $(x_1,x_2)^\top=(u_1-u_2,r_1-r_2)^\top$ is a particular solution of Eqs. (4.24). The evolution matrix in Eqs. (4.24) takes the form

$$\mathbf{M}=\begin{pmatrix}-a-\kappa & -b\\ -a & -b\end{pmatrix},$$

with $a=k_+(r_1+r_2)$ and $b=k_-+k_+(u_1+u_2)$. The associated eigenvalues are $\mu=-\lambda_\pm$ with

$$\lambda_\pm=\frac{1}{2}\left[a+b+\kappa\pm\sqrt{(a+b+\kappa)^2-4\kappa b}\right]>0,$$

and corresponding eigenvectors are

$$\mathbf{v}_+=(\lambda_+-b,a)^\top,\quad \mathbf{v}_-=(-b,\lambda_+-b)^\top.$$

Since were interested in the large κ limit, we will assume that $\kappa\geq a,b$. It follows that

$$\lambda_+\approx\kappa,\quad \lambda_-\approx\frac{b}{\kappa}, \tag{4.25}$$

and we can take $\mathbf{v}_+\approx(\lambda_+,a)^\top,\mathbf{v}_2\approx(-b,\lambda_+)^\top$. Diagonalizing Eqs. (4.24) by setting $\mathbf{y}=\mathbf{T}\mathbf{x}$ with $\mathbf{T}=(\mathbf{v}_1,\mathbf{v}_2)^\top$ then yields the following pair of uncoupled Langevin Eqs.

$$\frac{dy_1}{dt}=-\lambda_+y_1+\theta_0\lambda_+\xi(t) \tag{4.26a}$$

$$\frac{dy_2}{dt}=-\lambda_+y_2-\theta_0b\xi(t). \tag{4.26b}$$

It follows that [35]

$$\mathbb{E}[y_1^2]\leq\frac{\theta_0^2\lambda_+}{2},\quad \mathbb{E}[y_2^2]\leq\frac{\theta_0^2b^2}{\lambda_-}.$$

Now considering the inverse transform $\mathbf{x}=\mathbf{T}^{-1}\mathbf{y}$ for large κ, that is,

$$x_1\approx\frac{y_1}{\lambda_+}-\frac{a}{\lambda_+^2}y_2,\quad x_2\approx\frac{b}{\lambda_+^2}y_1+\frac{1}{\lambda_+}y_2,$$

we see obtain the approximate upper bounds

$$\mathbb{E}[x_1^2]\leq\frac{\theta_0^2}{2\lambda_+},\quad \mathbb{E}[x_2^2]\leq\frac{\theta_0^2b^2}{\lambda_-\lambda_+^2}.$$

Finally, since $(x_1,x_2)^\top=(u_1-u_2,r_1-r_2)^\top$ is a particular solution of Eqs. (4.24), we conclude that

$$\mathbb{E}[(u_1-u_2)^2]\leq\frac{\theta_0^2}{2\kappa},\quad \mathbb{E}[(r_1-r_2)^2]\leq\frac{\theta_0^2b}{2\kappa}.$$

We have used the approximations (4.25).

A similar argument can be applied for $N>2$ by choosing any pair $1\leq i,j\leq N$, $i<j$ and showing that

$$\mathbb{E}[(r_i-r_j)^2]+\mathbb{E}[(u_i-u_j)^2]\leq\frac{\theta_0^2(1+b)}{\kappa}.$$

Summing over i,j then yields

$$\mathbb{E}[\sum_{i<j}\|\mathbf{x}_i-\mathbf{x}_j\|^2]\leq\frac{N(N-1)\theta_0^2(1+b)}{2\kappa}.$$

It follows that for large κ,N, Eq. (4.22) holds with

$$\rho/N^2\sim\theta_0^2(1+b)/\kappa,$$

which converges to zero as $\kappa\to\infty$.

The suppression of receptor fluctuations for large coupling κ is further confirmed by carrying out simulations of the stochastic model given by Eqs. (4.11). Even for a relatively small population ($N=10$) it can be seen that fluctuations in the concentration $r_i(t)$ about the equilibrium state $r_{\rm eq}$ are negligible for large κ, see Fig. 10. Note that for simplicity, we take noise throughout the paper to be white noise. This means that even for sufficiently small noise intensities θ_0 and σ_0 there is a small but non-zero probability that a trajectory can become negative, see Fig. 10(a). A more realistic model would require some form of multiplicative noise to ensure that concentrations remain positive. However, this makes the analysis more difficult, without changing the basic results.

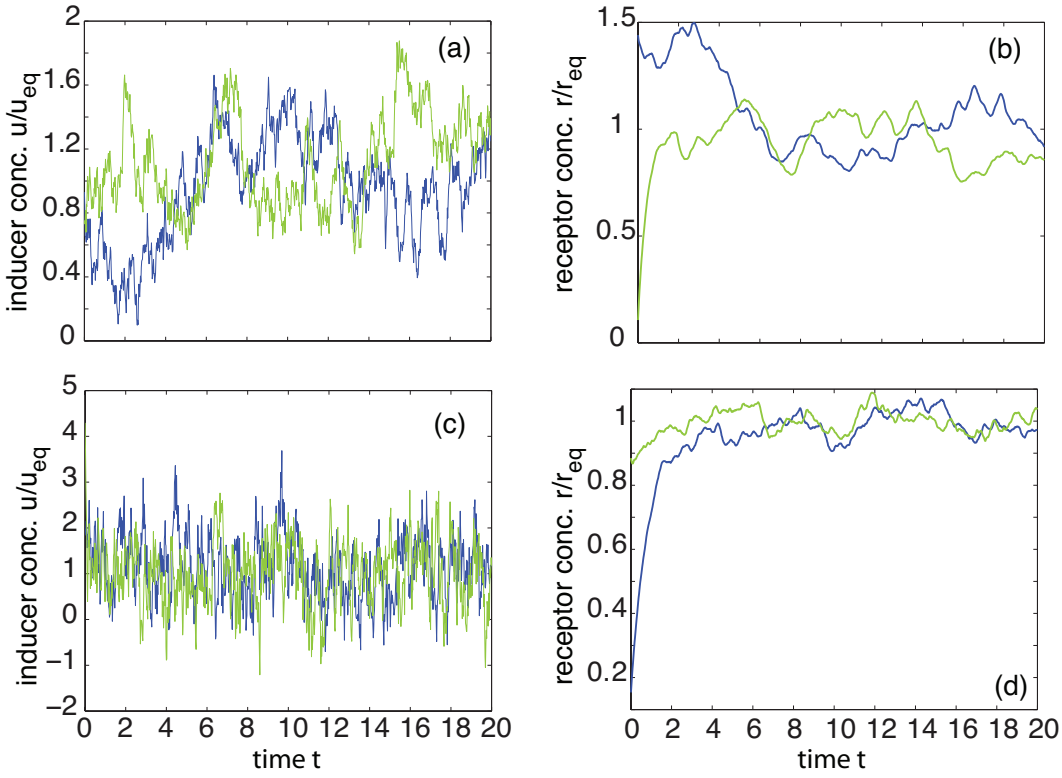

FIG. 10. (Color online) Plots of autoinducer and receptor concentrations for the stochastic quorum sensing model consisting of $N = 10$ coupled cells. The time evolution of two cells are represented by the green (light) and blue (dark) trajectories, respectively. (a,b) Solutions for $\kappa = 1$. (c,d) Solutions for $\kappa = 8$. Other parameter values are $k_- = k_+ = 1$, and $R_T = W_T = 1$, $\alpha = 0.05$ and $\theta_0 = 0.5$.

V. DISCUSSION

In this paper we investigated how collective cell behavior in a quorum sensing model system affects ultrasensitivity and noise amplification in a feedforward signal transduction pathway. The latter was taken to be a classical phosphorylation-dephosphorylation cycle, in which the ratio of kinases to phosphotases within each cell is controlled by the binding of autoinducers to their cognate receptor. We showed how global convergence of the quorum sensing network can greatly reduce the level of fluctuations in the number of kinases within a cell. Although we focused on one specific example of PdPCs, the results of our analysis should be applicable to other examples of switch-like biochemical networks.

Within the specific context of *V. harveyi* quorum sensing, we made a number of simplifications that warrant a closer look. First, we only considered a single signaling pathway, whereas *V. harveyi* and *V. cholerae* have several parallel pathways that converge to control downstream gene regulatory networks. It has been suggested that this "many-to-one" circuitry allows theses cells to survey heterogenous populations involving different bacterial species, and to program gene expression based on the make up of the population [30, 32]. Second, we ignored another potential source of switch-like behavior, involving the action of the small sRNAs Qrr1–Qrr5 [31]. Third, we neglected feedback pathways in which the downstream gene regulatory network controlled by the phosphorylation-dephopshorylation of LuxU modifies the rate of synthesis of the autoinducers. A number of feedback loops have recently been identified in *V. harveyi* and *V. cholerae*, and it has been suggested that they contribute to reducing the detrimental effects of sudden fluctuations in the environment [32].

ACKNOWLEDGEMENTS

PCB was supported by the National Science Foundation (DMS-1120327).

[1] C. Fuqua, S. C. Winans and E. P. Greenberg. Annu. Rev. Microbiol. **50** 727-751 (1996).

[2] D. G. Davies, M. R. Parsek, J. P. Pearson, B. H. Iglewski, J. W. Costerton and E. P. Greenberg. Science **280** 295-298 (1998).

[3] P. V. Dunlap J. Mol. Microbiol. Biotechnol. **1** 5-12 (1999).

[4] D. D H. Lenz, K. C. Mok, B. N. Lilley, R. V. Kulkarni, N. S. Wingreen and B. L. Bassler. Cell **118** 69-82 (2004).

[5] C. M. Waters and B. L. Basser. Annu. Rev. Cell Dev. Biol. **21** 319-346 (2005).

[6] L. R. Swem, D. L. Swem, N. S. Wingreen and B. L. Bassler. Cell **134** 461-473 (2008).

[7] Y. Wei, W. L. Ng, J. Cong and B. L. Bassler. Mol. Microbiol. **83** 1095-1108 (2012).

[8] T. Miyashiro, and E. G. Ruby. **84** 795-806 (2012).

[9] I. D. Couzin. Trends. Cogn. Sci. **13** 36-43 (2009).

[10] S. James, P. Nilsson, G. James, S. Kjelleberg and T. Fagerstrom. J. Mol. Biol. **296** 1127-1137 (2000).

[11] J. P. Ward, J. R. King, A. J. Koerber, P. Williams, J. M. Croft and R. E. Sockett. IMA J. Math. Appl. Med. **18** 263-292 (2001).

[12] J. D. Dockery and J. P. Keener. Bull. Math. Biol. **63** 95-116 (2001).

[13] K. Anguige, J. R. King and J. P. Ward. Math.Biosci. **203** 240-276 (2006).

[14] S. De Monte, F. dOvidio, S. Dano and P. G. Sorensen. Proc. Natl. Acad. Sci. USA **104** 18377-18381 (2007).

[15] A. B. Goryachev. WIREs Syst. Biol. Med. **1** 45-60 (2009).

[16] C. Garde, T. Bjarnsholt, M. Givskov, T. H. Jakobsen, M. Hentze, A. Claussen, K. Sneppen, J. Ferkinghoff-Borg and T. Sams. J. Mol. Biol. **396** 849-857 (2010).

[17] W-Y Chiang, Y-X Li and P-Y Lai. Phys. Rev. E **84** 041921 (2011) .

[18] P. Mina, M. di Bernardo, N. J. Savery, K Tsaneva-Atanasova. J. Roy. Soc. Interface **10** 20120612 (2013).

[19] J. Muller, C. Kuttler, B. A. Hense, M. Rothballer and A. Hartmann. J. Math. Biol., **53** 672-702 (2006).

[20] I. Klapper and J. Dockery. SIAM Rev. **52** (2010).

[21] J. Muller and H. Uecker. with localization, J. Math. Biol. **67** 1023-1065 (2013).

[22] J. Gou and M. J. Ward. J. Nonlin. Sci. (2016).

[23] A. Goldbeter and D. E. Koshland. Proc. Natl. Acad. Sci. USA **78** 6840-6844 (1981).

[24] O. G. Berg, J. Paulsson and M. Ehrenberg. Biophys. J. **79** 12281236 (2000).

[25] H. Qian. Biophys. Chem. **105** 585593 (2003).

[26] H. Ge and M. Qian. J. Chem. Phys. **129** 015104 (2008)

[27] H. Qian. Annu. Rev. Biophys. **41**, 179-204 (2012).

[28] G. Russo and J. J. E. Slotine. Phys. Rev. E **82** 041919 (2010).

[29] W. Lohmiller and J. J. E. Slotine. Automatica **34** 683-696 (1998).

[30] S. A. Jung, L. A. Hawver and W-L Ng. Curr. Genet. **62** 255 (2016).

[31] G. A. M. Hunter, F. Guevara Vasquez and J. P. Keener. Phys. Biol. **10** 046007 (2013).

[32] W. L. Ng and B. L. Bassler Annu. Rev. Genet. **41** 197-222 (2009).

[33] T. Shibata and K. Fujimoto. Proc. Natl. Acad. Sci. USA **100** 331-336 (2005).

[34] J. Levine and H. Y. Kueh and L. Mirny. Biophys. J. **92** 4473-4481 (2007).

[35] N. Tabareau, J. J. Slotine and Q-C Pham. PLoS Comput. Biol. **6** e1000637 (2010).

[36] A. B. Goryachev, D-J Toh, K. B. Wee, T. Lee, H-B Zhang and L-H Zhang. PLoS Comput. Biol. **1** e37 (2005).

[37] M. Weber and J. Buceta. BMC Syst. Biol. **7** 6 (2013).

[38] P. C. Bressloff. *Stochastic processes in Cell Biology*. Springer (2014)